Bulgarian Chemical Communications, Volume 50, Special issue H (pp. 80–86) 2018

Nanosized mesoporous titania composites promoted with ceria and zirconia as catalysts for ethyl acetate oxidation: effect of preparation procedure

G. S. Issa[1]*, M. D. Dimitrov[1], D. G. Kovacheva[2], T. S. Tsoncheva[1]

[1] *Institute of Organic Chemistry with Centre of Phytochemistry, Bulgarian Academy of Sciences, Acad. G. Bonchev St., Bldg. 9, 1113 Sofia, Bulgaria,*

[2] *Institute of General and Inorganic Chemistry, Bulgarian Academy of Sciences, Acad. G. Bonchev St., Bldg. 11, 1113 Sofia, Bulgaria*

Received: January 15, 2018; Revised: March 07, 2018

The aim of the current investigation was to develop a series of titania-based nanosized mesoporous binary materials promoted with Ce and Zr and to test them as catalysts for total oxidation of ethyl acetate. Metal oxide materials were synthesised by template-assisted hydrothermal approach and homogeneous precipitation with urea. The main aspect of the study was to find a relationship between preparation procedure and structure, texture, surface, and catalytic properties of the obtained materials. These materials were characterised by low temperature nitrogen physisorption, XRD, Raman and UV-Vis spectroscopy, and temperature-programmed reduction with hydrogen. The hydrothermal method enabled formation of mesoporous materials of better homogeneity as compared to urea-synthesised counterparts where certain microporosity was registered as well. Doping agents affected preparation procedures. Improved texture parameters of ZrTi binary oxides obtained by the hydrothermal technique facilitated their catalytic activity as compared to urea analogues. Just an opposite effect of preparation was observed for CeTi materials.

Key words: mesoporous catalysts, Ce-pomoted titania, Zr-promoted titania, ethyl acetate oxidation.

INTRODUCTION

Volatile organic compounds (VOCs) are important environmental pollutants produced from refineries, fuel storage and loading operations, motor vehicles, solvent cleaning, printing and painting operations [1]. VOCs are regarded as critical precursors for the potential formation of tropospheric ozone and photochemical smog. Examples of common VOCs are ethyl acetate, benzene, toluene, acetone, and ethanol [2]. In particular, ethyl acetate is one of the most common VOCs, used in printing operations, glues, and nail polish removers, often employed as a model compound for VOCs oxidation [3,4]. Catalytic oxidation seems to be very promising for VOCs elimination. Practical realisation of each of these catalytic processes requires the development of effective catalysts remarkable not only for their activity, stability, and selectivity, but for their low cost and ability to operate at relatively low temperatures. In recent years, efforts in this direction were focused on obtaining new porous materials based on transition metal oxides [5]. Improved methods for their synthesis have led to new materials of different morphology, high specific surface area, and well developed porous structure. These materials contain pores of different size, shape, and topology, and in some cases functionalise the surface of the metal oxide to acquire tunable surface properties [5−10]. Moreover, multicomponent nanosized metal oxide materials are subject of even greater interest for improving their properties via exhibited synergism among the individual components, i.e. one of the metal oxides may change the properties of another one because of electronic and structural impacts. Recently titania has received much attention owing to its non-toxicity, chemical and biological inertness, availability, and low cost. Preparation of nanodisperse mesoporous titania and its doping with different metal oxides provide good opportunities not only for improved catalytic behaviour, but also for formation of new stable composites, which could manifest completely different physicochemical and catalytic properties [6]. Titania-ceria materials represent undoubted interest due to an important role of the cerium dopant to decrease particle size, and to cause a strong effect on metal oxide reducibility, high degree of synergistic interaction between components, and favourable modification of structural and catalytic properties [8]. It has been established that isomorphous substitution of cerium ions into the TiO_2 lattice generates oxygen vacancies, which stabilise the anatase phase, increases the specific surface area and the dispersion of the metal oxide particles [8]. It has been demonstrated that addition

* To whom all correspondence should be sent
E-mail: *Issa@abv.bg*

of zirconia to titania can significantly increase surface acidity by formation of OH groups and the acid-base properties can be substantially influenced by the Ti/Zr ratio [9]. It has been shown that individual components in these binary oxides interact to form $ZrTiO_4$ [9]. The aim of this investigation is to obtain nanosized mesoporous ceria-titania and zirconia-titania binary materials and to test them as catalysts for complete oxidation of ethyl acetate. The materials were synthesised by template-assisted hydrothermal approach (HT) and homogeneous precipitation with urea (U). A principal aspect in the study was to find a relationship between preparation procedure and structure, texture, and catalytic properties of the obtained materials.

EXPERIMENTAL

Mono and bi-component titania, ceria, and zirconia materials were synthesised by hydrothermal procedure (HT) using cetyltrimethylammonium bromide (CTAB) as a structure-directing template [10] and by homogeneous precipitation with urea (U) [11]. Samples were denoted as xCeyTi M and xZryTi M, where x/y was metal to mol ratio, which in the bi-component samples was 5:5, and M was the preparation method used. Textural characteristics were acquired from nitrogen adsorption-desorption isotherms measured at 77 K using a Coulter SA3100 instrument. Powder X-ray diffraction patterns were collected on a Bruker D8 Advance diffractometer with Cu Kα radiation using a LynxEye detector. UV-Vis spectra were recorded on a Jasco V-650 UV-Vis spectrophotometer. Raman spectra were registered on a DXR Raman microscope applying a 780-nm laser. TPR/TG analyses were performed on a Setaram TG92 instrument in a flow of 50 vol.% H_2 in Ar. Catalytic oxidation of ethyl acetate (EA) was conducted in a flow type reactor with a mixture of EA and air. Gas chromatographic analyses were made on a HP 5890 apparatus using carbon-based calibration

RESULTS AND DISCUSSION

Table 1 presents nitrogen physisorption data on ceria-titania and zirconia-titania materials. Addition of zirconia or ceria to TiO_2 led to an increase of both specific surface area and pore volume. The urea-prepared materials exhibited up to 5 times lower values of pore volume as compared to the HT samples due to mainly smaller mesopores and to a certain amount of micropores because of interparticle interaction. The best texture characteristics were registered for 5Zr5Ti obtained by hydrothermal method. Thus, the development of mesoporous structure was strongly dependent on the preparation technique. The latter was mostly controlled by the organic template during the hydrothermal procedure and by interparticle interaction on using urea for homogeneous precipitation. These effects were better pronounced for the binary oxides.

Table 1. Nitrogen physisorption and XRD data of CeTi and ZrTi materials.

Sample	Phase composition	Unit cell parameters, Å	Cristallite size, nm	S_{BET}, m^2g^{-1}	V_t, cm^3g^{-1}
TiO_2 HT	anatase, syn	3.7861	17	85	0.29
	tetragonal body-centred I41/amd	9.493			
TiO_2 U	anatase, syn	3.7855	13	97	0.19
	tetragonal body-centred I41/amd	9.507			
CeTi HT	cerium oxide	5.403	12	99	0.45
	face-centred cubic Fm-3m				
CeTi U	anatase, syn	3.770	5	117	0.30
	tetragonal body-centred I41/amd	9.51	7		
	cerium oxide face-centred cubic Fm-3m	5.401			
CeO_2 HT	cerium oxide	5.416	10	46	0.26
	face-centred cubic Fm-3m				
CeO_2 U	cerium oxide face-centred cubic Fm-3m	5.4144	13	76	0.07
ZrTi HT	amorphous			248	0.69
ZrTi U	amorphous			204	0.16
ZrO2 HT	tetragonal ZrO_2	3.591	13	67	0.32
		5.183			
	monoclinic ZrO_2	5.303	14		
		5.163			
		5.197			
		β = 99.17			
ZrO2 U	tetragonal ZrO_2	3.6006	30	2	0.02
		5.1859			

Figure 1 displays XRD patterns of both series of samples, while phase composition, unit cell parameters, and average crystallite size are shown in Table 1. The diffraction peaks in the pattern of TiO_2 HT and TiO_2 U at 25.5°, 38.2°, 47.8°, 54.3°, and 62.8° 2θ are indexed to a pure anatase phase of titania with average crystallite size of about 8 nm and 13 nm, respectively (Table 1) [6].

The XRD patterns of both CeO_2 samples consist of intensive diffraction peaks at 28.5°, 33.1°, 47.6°, 56.5°, and 59.2° 2θ. They are indexed to a face-centred fluorite type structure [7] with average crystallite size of 10−13 nm. Ceria with average crystallite size of 12 nm was only registered for CeTi HT, while a mixture of anatase and ceria with average crystallite size of 5 and 7 nm, respectively, was found for CeTi U. A slight decrease in unit cell parameters accompanied with an increase of the ceria average particle size as compared to the individual CeO_2 sample was observed. This could be evidence for a Ce-O-Ti interface layer formation *via* incurporation of smaller Ti^{4+} ions in the ceria [8]. The XRD patterns of pure zirconia samples showed strong reflections at 2θ = 30.17°, 49.81°, 50.07°, and 60.15° that are typical of the crystalline planes of tetragonal zirconia phase. Additional reflections at 2θ = 28.19°, 31.48°, 34.19°, 45.52°, 49.26°, and 54.1° for ZrO_2 HT correspond to the crystalline planes of monoclinic zirconia (Figure 1b) [9]. The average crystallite size of zirconia was 13−14 nm for the hydrothermally obtained sample and about 30 nm for the urea one, which indicates that the former technique is more appropriate to prepare nanodispersed zirconia. Despite the preparation method used, XRD patterns of mixed ZrTi oxides demonstrate a broad hump, which is typical of amorphous materials. Here, a plateau in the XRD patterns indicates the formation of very finely dispersed oxides, which well correlates with an extremely high surface area for these materials (Table 1).

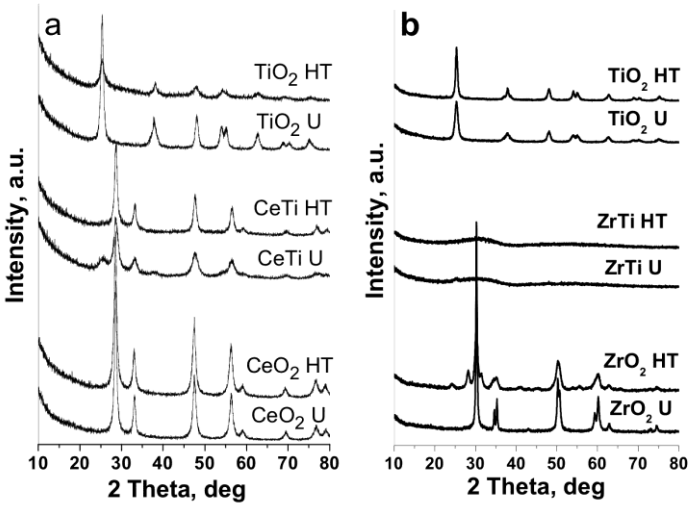

Fig. 1. XRD patterns of CeTi (a) and ZrTi (b) materials.

The UV-Vis spectra of both series of samples prepared by hydrothermal and urea treatment are displayed in Figures 2a and 2b. A strong absorption feature in the spectra of both titania samples at 350 nm is typical of anatase [12], which is also consistent with the XRD data. The UV-Vis spectra of pure CeO_2 HT and CeO_2 U demonstrate absorption at 240, 285, and 330 nm which can be attributed to $O_2 \rightarrow Ce^{3+}$ charge transfer (CT), $O_2 \rightarrow Ce^{4+}$ CT, and interband transitions, respectively (Fig. 2a) [13]. The latter band is related to defect lattice sites as well. A shift of the main absorption edges with both individual cerium oxides indicates higher dispersion for the hydrothermally obtained materials.

Changes in the 350–500 nm region of both bicomponent CeTi materials confirm the assumption made above of strong interaction between metal ions and/or increase in metal oxide dispersion (Fig. 2a). The spectra of both zirconia samples show two absorption bands at around 208 and 230 nm as expected for m-ZrO_2 (Fig. 2b). The second feature in the spectra at absorption threshold position around 320 nm reveals coexistence of t-ZrO_2 [14]. In consistence with the XRD data (Fig. 1b, Table 1) a slight red shift in the position of the main feature for ZrO_2 HT and appearance of additional absorption bands at about 300 and 450 nm could be assigned to higher dispersion of the zirconia phase. The overall absorption of mixed ZrTi materials is significantly higher as compared to pure zirconia samples. The observed features could not be simply assigned to superposition of the spectra of the single metal oxides. According to Ref. [15] and in consistence with nitrogen physisorption and XRD

results these features could be attributed to formation of amorphous phase and modification of the titania lattice because of Zr^{4+} ion incorporation.

Figure 3 gives Raman spectra of CeTi materials prepared by various procedures. Raman shifts at 143, 195, 396, 514, and 637 cm^{-1} in the spectra of both titania samples demonstrate presence of pure anatase phase (Fig. 3a) [16]. Anatase bands at 396 and 639 cm^{-1} are ascribed to Ti−O stretching vibrations and to Eg mode of O−Ti−O bending vibration, respectively [16]. Only one Raman-active F2g mode, centred at about 463 cm^{-1}, which is typical of cubic structure, was detected for both ceria materials (Fig. 3b) [8,17]. The appearance of second less prominent and broad band at about 600 cm^{-1} is usually assigned to defect-induced longitudinal optical mode of ceria due to formation of oxygen vacancies [17]. The main Raman active mode is broader for ceria prepared by urea technique, which in accordance with the XRD data could be due to a decrease of crystallite size.

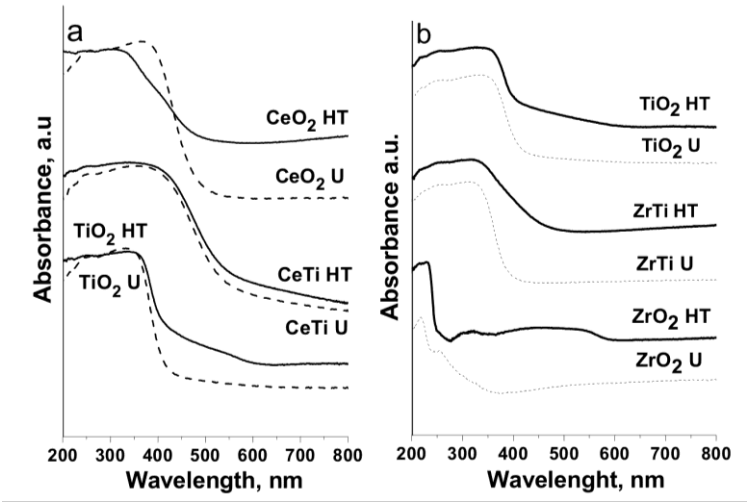

Fig. 2. UV-Vis spectra of CeTi (a) and ZrTi (b) materials, prepared by urea (dash lines) and template hydrothermal (solid lines) methods.

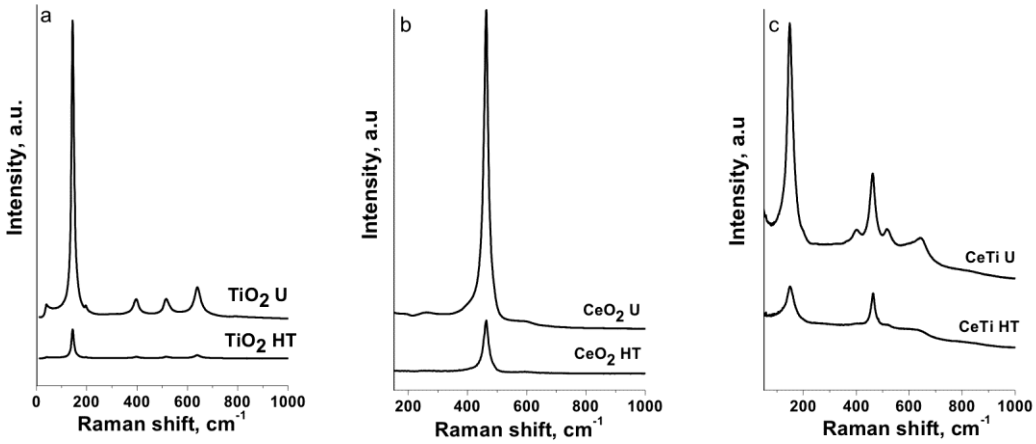

Fig. 3. Raman spectra of titania (a), ceria (b), and CeTi (c) materials.

The Raman spectra of binary oxides reveal that they represent a mixture of ceria and anatase phases, the latter being of higher amount for the urea-prepared sample (Fig. 3c), which is in agreement with the XRD data. A slight blue shift of the Raman E1g mode to 150 cm^{-1} could indicate changes in the environment of titanium ions in anatase lattice. A shift of the main signal to higher wavenumber values with the bi-component samples is due to shortening of the Ce−O bond because of incorporation of titanium ions into the cerium oxide lattice. E1g band widening could be attributed to a decrease of crystallite size, which is in accordance with reported XRD and UV-Vis data.

Figure 4 shows Raman spectra of the obtained ZrTi samples. The bands at 142, 270, 317, 458, and 643 cm^{-1} in both spectra of ZrO_2 are compatible to tetragonal zirconia (Fig. 4a) [18]. In consistence with the XRD study additional Raman bands at 176, 192, 478, and 612 cm^{-1} in the spectrum of ZrO_2 HT

indicate co-existence of monoclinic zirconia.

Not well defined peaks are visible in the Raman spectra of ZrTi samples, which can be attributed to the amorphization of the crystal structure and increased concentration of defects arising from the incorporation of zirconium ions in titania and/or to the significant particle size decrease (Fig. 4b). The observed slight shifting and broadening of the main Raman-active mode of anatase accompanied with a decrease in its intensity could be assigned to metal oxide bonds shortening and formation of smaller crystallites with defect structure due to the replacement of titanium ions with zirconium ones.

TPR-TG profiles of hydrothermally synthesised and urea-precipitated CeTi samples were compared in the 500–750 K region (not shown). A weight loss agreed with reduction of Ce^{4+} to Ce^{3+}, being about 10 and 4% for CeO_2 HT and CeO_2 U, respectively. Reduction started at a lower temperature with the bi-components samples and the effects were larger in comparison with the pure ceria samples. In accordance with other physicochemical measurements, an increased mobility of lattice oxygen in these materials could be due to increased dispersion as well as owing to distortion of the ceria lattice during titanium incorporation. The reduction behaviour of the mixed materials was not simply related to their specific surface area. Thus, a facile reduction of the hydrothermally obtained samples is probably related to their higher dispersion, well-developed mesoporous structure, and homogeneous phase composition. Not all zirconia-containing samples manifested reduction ability in the studied temperature interval.

Figure 5 gives temperature dependencies of total oxidation of EA on various materials. Temperatures at which a 50% conversion over various samples was achieved are compared in Table 2. Beside CO_2, which is the most important product of EA oxidation, (Fig. 5b), ethanol, acetaldehyde, acetic acid, and ethene were also registered as by-products. All materials were catalytically active above 500−525 K, and 80−100% conversion was achieved at 600−670 K

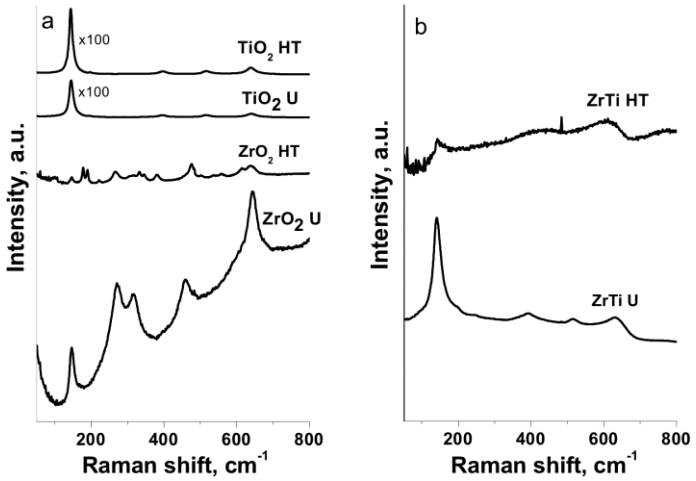

Fig. 4. Raman spectra of zirconia and titania (a) and ZrTi (b) materials.

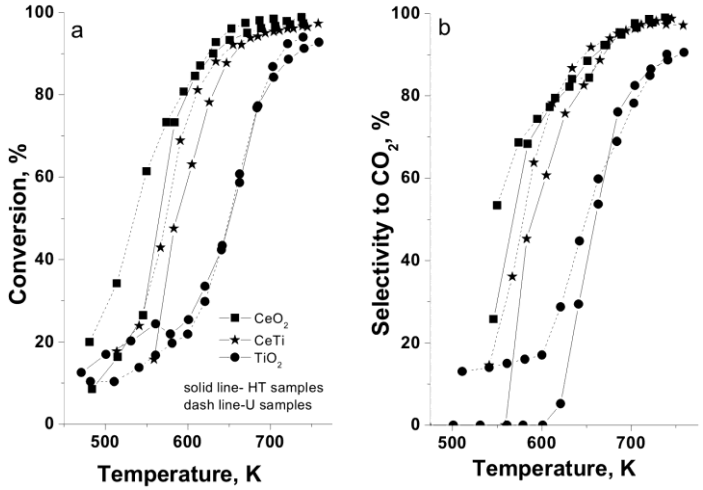

Fig. 5. Ethyl acetate conversion (a) and selectivity to CO_2 (b) of CeTi materials.

(Fig. 5a). Titania exhibited a notably low catalytic (Table 2) activity combined with high ability to form by-products, mainly acetaldehyde, ethanol, and ethane. Just the opposite, both mono-component ceria samples manifested high activities, but low selectivity to CO_2 due to the formation of ethanol as by-product (Table 2). Ceria-titania binary materials possessed a lower catalytic activity as compared to pure CeO_2 (Table 2, Fig. 5a) and a higher selectivity for total oxidation of ethyl acetate to CO_2 which could be due to improved redox ability. A common feature was a higher activity of all urea-precipitated materials as compared to their hydrothermally prepared analogues.

Table 2. Temperatures for 50% conversion of ethyl acetate and specific catalytic activity for CeTi and ZrTi materials

Sample	$T_{50\%}$, K	SA, EA mol.m^{-2}	Sample	$T_{50\%}$, K	SA, EA mol.m^{-2}
TiO_2 HT	660	0.29	TiO_2 HT	650	0.56
TiO_2 U	651	0.23	TiO_2 U	650	0.52
CeTi HT	586	0.60	ZrTi HT	629	0.26
CeTi U	574	0.65	ZrTi U	660	0.21
CeO_2 HT	560	1.74	ZrO_2 HT	650	0.78
CeO_2 U	535	1.09	ZrO_2 U	713	1.7

To ignore any effect of different specific surface area of the samples (Table 1), specific catalytic activity (SA) was calculated as conversion at a selected temperature per unit surface area (Table 2). Here, the urea samples exhibited lower or similar SA to the HT analogues indicating that the observed catalytic behaviour was strongly related to increased surface area during urea synthesis.

Figure 6a presents temperature dependencies of catalytic activity in ethyl acetate oxidation for the ZrTi materials. The mono-component zirconia sample exhibited the lowest activity, a relatively low selectivity of ethyl acetate oxidation to CO_2, and formation of significant amount of ethanol as by-product (Fig. 6b). This was probably due to a higher hydrolysis degree of ethyl acetate on the acid/base sites of zirconia, which is generally assumed as a first step in ethyl acetate oxidation [19]. The bicomponent samples manifested a higher catalytic activity and CO_2 selectivity than the corresponding mono-component materials (Fig. 6a). Taking into account the physicochemical data, we ascribe this result to a specific interaction between the individual oxides and increased surface area of the mixed oxide materials. The catalytic activity of the hydrothermally prepared composites was higher as compared to the urea samples.

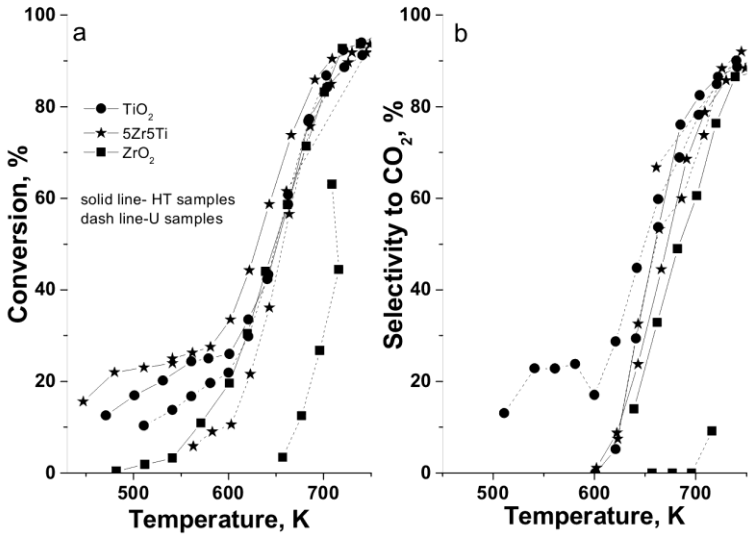

Fig. 6. Ethyl acetate conversion (a) and selectivity to CO_2 (b) of ZrTi materials.

The binary materials showed a lower specific catalytic activity as compared to the individual metal oxides (Table 2). In accordance with the XRD, UV-Vis, and Raman data, significant changes in the nature of the active sites due to incorporation of zirconium ions into titania lattice could be proposed and this could be successfully controlled by the preparation procedure used.

CONCLUSIONS

Highly dispersed titania doped with ceria and zirconia materials were successfully prepared by using a template-assisted hydrothermal procedure and homogeneous precipitation with urea. The effect of the preparation technique on the properties of the obtained binary titania-based materials was depend-

ent on the nature of dopant. In the case of ceria doping, the template-assisted hydrothermal synthesis facilitated formation of more homogeneous materials, but exhibiting lower dispersion and lower specific surface area. This provided a lower catalytic activity for complete oxidation of ethyl acetate. In contrast, the zirconia dopant significantly improved the texture characteristics of titania and enhanced the catalytic activity of hydrothermally synthesised materials.

Acknowledgements: *Financial support by project DM-09/4/2016 is gratefully acknowledged. A bilateral project between Bulgarian Academy of Sciences and Czech Academy of Sciences is also acknowledged. The authors thank V. Stengl, J. Henych, and M. Slusna from Institute of Inorganic Chemistry of the Czech Academy of Sciences for Raman spectra and nitrogen physisorption measurements and synthesis of urea samples.*

REFERENCES

1. W. G. Tucker, Digital Engineering Library, @ McGraw-Hill, New York, 2004.
2. F. I. Khan, A.K. Ghoshal, *J. Loss Prev. Process Ind*., **13**, 527 (2000).
3. S. Akram, Z. Wang, L. Chen, Q. Wang, G. Shen, N. Han, Y. Chen, G. Ge, *Catal. Commun*., **73,** 123 (2016).
4. S. Carabineiro, M. Konsolakis, G. Marnellos, M. Asad, O. Soares, P. Tavares, M. Pereira, J. Órfão, J. Figueiredo, *Molecules*, **21,** 644 (2016).
5. S. Yuesong , Z. Dahai, Y. Bo, N. Songbo, Z. Shemin, *J. Rare Earths*, **30**, 431 (2012).
6. M. Altomare, M. Dozzi, G. Chiarello, A. Paola, L. Palmisano, E. Selli, *Catal. Today*, **252**, 184 (2015).
7. D. W. Wheeler, I. Khan, *Vib. Spectrosc*., **70**, 200 (2014).
8. J. Fang, X. Bi, D. Si, Z. Jiang, W. Huang, *Appl. Surf. Sci*., **253**, 8952 (2007).
9. B. Neppolian, Q. Wang, H. Yamashita, H. Choi, *Appl. Catal. A: Gen*., **333,** 264 (2001).
10. T. Tsoncheva, I. Genova, M. Dimitrov, E. Sarcadi-Priboczki, A. M. Venezia, D. Kovacheva, N. Scotti, V. dal Santo, *Appl. Catal. B: Environ.,* **165**, 599 (2015).
11. J. Subrt, V. Stengl, S. Bakardjieva, L. Szatmary, *Powder Technol*., **169**, 33 (2006).
12. M. N. Iliev, V. G. Hadjiev, A. P. Litvinchuk, *Spectroscopy*, **64**, 148 (2013).
13. A. Kambolis, H. Matralis, A. Trovarelli, Ch. Papadopoulou, *Appl. Catal. A: Gen*., **377**, 16 (2010).
14. S. Damyanova, B. Pawelec, K. Arishtirova, M. V. Martinez Huerta, J. L. G. Fierro, *Appl. Catal. A: Gen*., **337,** 86 (2008).
15. M. Fernàndez-García, A. Martínez-Arias, J. C. Hanson, J. A. Rodriguez, *Chem. Rev*., **104**, 4063 (2004).
16. K. C. Silva, P. Corio, J. J. Santos, *Vib. Spectrosc*., **86**, 103 (2016).
17. D. R. Sellick, A. Aranda, T. García, J. M. López, B. Solsona, A. M. Mastral, D. J. Morgan, A. F. Carley, S. H. Taylo, *Appl. Catal. B: Environ*., **132–133**, 98 (2013).
18. W. Zhu, N. Sugano, G. Pezzotti, *J. Biomed. Opt*., **18**, 127 (2013).
19. P.-O. Larsson, A. Andersson, *Appl. Catal. B: Environ*., **24**, 175 (2000).

ВЛИЯНИЕ НА МЕТОДА НА ПОЛУЧАВАНЕ ВЪРХУ ФОРМИРАНЕТО НА НАНОСТРУКТУРИРАНИ МЕЗОПОРЕСТИ CeO_2-TiO_2 И ZrO_2-TiO_2 КАТАЛИЗАТОРИ ЗА ПЪЛНО ОКИСЛЕНИЕ НА ЕТИЛАЦЕТАТ

Г. С. Исса[1], М. Д. Димитров[1], Д. Г. Ковачева[2], Т. С. Цончева[1]

[1] *Институт по органична химия с Център по фитохимия, БАН, 1113 София, България*
[2] *Институт по обща и неорганична химия, БАН, 1113 София, България*

Постъпила на 15 януари 2018 г.; Преработена на 7 март 2018 г.

(Резюме)

Цел на настоящото изследване е получаване на наноразмерни мезопорести смесени материали на основата на промотиран с Ce и Zr титанов оксид и тестването им като катализатори в реакция на пълно окисление на етилацетат. Получените оксиди бяха синтезирани чрез хидротермален синтез в присъствието на органичен темплейт и хомогенно утаяване с карбамид. Основен аспект в изследването е изясняване на връзката между използвания метод на получаване и текстурата, структурата и окислително-редукционните свойства на получените материали. Образците бяха характеризирани чрез физична адсобция на азот, рентгеноструктурен анализ, UV-Vis и Раманова спектроскопия, както и температурно програмирана редукция. Хидротермалният метод благоприятства формирането на мезопорести и по-хомогенни материали в сравнение със синтезираните с карбамид образци, където се регистрира и известна микропористост. Ефектът от процедурата на получаване зависи от вида на металооксидната добавка към TiO_2. Подобрените текстурни характеристики на смесените ZrTi оксиди, получени чрез хидротермален метод благоприятстват тяхната каталитична активност в сравнение с получените с карбамид аналози. Точно обратният ефект се наблюдава при CeTi материалите.